

**AFRL-ML-WP-TP-2006-477**

**COMPARISON OF X-RAY,  
MILLIMETER WAVE,  
SHEAROGRAPHY AND THROUGH-  
TRANSMISSION ULTRASONIC  
METHODS FOR INSPECTION OF  
HONEYCOMB COMPOSITES  
(PREPRINT)**



**M.A. Abou-Khousa, A. Ryley, S. Kharkovsky, R. Zoughi,  
D. Daniels, N. Kreitingner, and G. Steffes**

**AUGUST 2006**

**Approved for public release; distribution is unlimited.**

**STINFO COPY**

**The U.S. Government is joint author of this work and has the right to use, modify,  
reproduce, release, perform, display, or disclose the work.**

**MATERIALS AND MANUFACTURING DIRECTORATE  
AIR FORCE RESEARCH LABORATORY  
AIR FORCE MATERIEL COMMAND  
WRIGHT-PATTERSON AIR FORCE BASE, OH 45433-7750**

<b>REPORT DOCUMENTATION PAGE</b>				<i>Form Approved</i> OMB No. 0704-0188	
The public reporting burden for this collection of information is estimated to average 1 hour per response, including the time for reviewing instructions, searching existing data sources, gathering and maintaining the data needed, and completing and reviewing the collection of information. Send comments regarding this burden estimate or any other aspect of this collection of information, including suggestions for reducing this burden, to Department of Defense, Washington Headquarters Services, Directorate for Information Operations and Reports (0704-0188), 1215 Jefferson Davis Highway, Suite 1204, Arlington, VA 22202-4302. Respondents should be aware that notwithstanding any other provision of law, no person shall be subject to any penalty for failing to comply with a collection of information if it does not display a currently valid OMB control number. <b>PLEASE DO NOT RETURN YOUR FORM TO THE ABOVE ADDRESS.</b>					
<b>1. REPORT DATE (DD-MM-YY)</b> August 2006		<b>2. REPORT TYPE</b> Conference Paper Preprint		<b>3. DATES COVERED (From - To)</b> 01/01/2005 – 12/31/2005	
<b>4. TITLE AND SUBTITLE</b> COMPARISON OF X-RAY, MILLIMETER WAVE, SHEAROGRAPHY AND THROUGH-TRANSMISSION ULTRASONIC METHODS FOR INSPECTION OF HONEYCOMB COMPOSITES (PREPRINT)				<b>5a. CONTRACT NUMBER</b> FA8650-04-C-5704	
				<b>5b. GRANT NUMBER</b>	
				<b>5c. PROGRAM ELEMENT NUMBER</b> 62112F	
<b>6. AUTHOR(S)</b> M.A. Abou-Khousa, A. Ryley, S. Kharkovsky, and R. Zoughi (University of Missouri-Rolla) D. Daniels, N. Kreitinger, and G. Steffes (AFRL/MLLP)				<b>5d. PROJECT NUMBER</b> 2510	
				<b>5e. TASK NUMBER</b> 00	
				<b>5f. WORK UNIT NUMBER</b> 00	
<b>7. PERFORMING ORGANIZATION NAME(S) AND ADDRESS(ES)</b> University of Missouri-Rolla Applied Microwave Nondestructive Testing Laboratory (amntl) Electrical and Computer Engineering Dept. 224 Emerson Electric Co. Hall 1870 Miner Circle Rolla, MO 65409-0040				<b>8. PERFORMING ORGANIZATION REPORT NUMBER</b>	
Nondestructive Evaluation Branch (AFRL/MLLP) Metals, Ceramics and NDE Division Materials and Manufacturing Directorate Air Force Research Laboratory Air Force Materiel Command Wright-Patterson AFB, OH 45433-7750					
<b>9. SPONSORING/MONITORING AGENCY NAME(S) AND ADDRESS(ES)</b> Materials and Manufacturing Directorate Air Force Research Laboratory Air Force Materiel Command Wright-Patterson AFB, OH 45433-7750				<b>10. SPONSORING/MONITORING AGENCY ACRONYM(S)</b> AFRL-ML-WP	
				<b>11. SPONSORING/MONITORING AGENCY REPORT NUMBER(S)</b> AFRL-ML-WP-TP-2006-477	
<b>12. DISTRIBUTION/AVAILABILITY STATEMENT</b> Approved for public release; distribution is unlimited.					
<b>13. SUPPLEMENTARY NOTES</b> The U.S. Government is joint author of this work and has the right to use, modify, reproduce, release, perform, display, or disclose the work. Conference paper submitted to the Proceedings of the 33rd Annual Review of Progress in Quantitative Nondestructive Evaluation (QNDE 2006), published by the American Institute of Physics. This is the best quality of this paper available. PAO Case Number: AFRL/WS 06-2123, 30 Aug 2006.					
<b>14. ABSTRACT</b> Honeycomb composites are increasingly finding utility in a variety of environments and applications, such as structural components, radomes, etc. In-service and environmental stresses can produce unwanted flaws that adversely affect the structural integrity and functionality of these composites. These flaws may be in the forms of disbonds, delaminations, impact damage, crushed honeycomb, moisture intrusion, internal cracks, etc. There are several nondestructive testing (NDT) methods that may be used to inspect these composites for the presence and evaluation of these flaws. Such NDT methods include X-Ray computed tomography, near-field millimeter wave, shearography, and ultrasonic testing. To assess the capabilities of these methods for honeycomb composite inspection, two honeycomb composites panels were produced with several embedded flaws primarily representing planar disbonds at various levels within the thickness of the panels and with different shapes. Subsequently, the aforementioned NDT methods were used to produce images of the two panels. This paper presents the results of these investigations and a comparison among the capabilities of these methods.					
<b>15. SUBJECT TERMS</b> honeycomb composite, microwave and millimeter wave, nondestructive testing (NDT), shearography, through-transmission ultrasound, X-ray computed tomography					
<b>16. SECURITY CLASSIFICATION OF:</b>			<b>17. LIMITATION OF ABSTRACT:</b> SAR	<b>18. NUMBER OF PAGES</b> 16	<b>19a. NAME OF RESPONSIBLE PERSON (Monitor)</b> Gary Steffes <b>19b. TELEPHONE NUMBER (Include Area Code)</b> N/A
<b>a. REPORT</b> Unclassified	<b>b. ABSTRACT</b> Unclassified	<b>c. THIS PAGE</b> Unclassified			

# COMPARISON OF X-RAY, MILLIMETER WAVE, SHEAROGRAPHY AND THROUGH-TRANSMISSION ULTRASONIC METHODS FOR INSPECTION OF HONEYCOMB COMPOSITES

M.A. Abou-Khousa<sup>1</sup>, A. Ryley<sup>1</sup>, S. Kharkovsky<sup>1</sup>, R. Zoughi<sup>1</sup>,  
D. Daniels<sup>2</sup>, N. Kreitinger<sup>2</sup> and G. Steffes<sup>2</sup>

<sup>1</sup>Applied Microwave Nondestructive Testing Laboratory (*amntl*)  
Electrical and Computer Engineering Department  
University of Missouri-Rolla  
Rolla, MO 65409

<sup>2</sup>Air Force Research Laboratory (AFRL)  
Materials and Manufacturing Directorate  
2230 Tenth Street, Ste. 1  
Wright-Patterson AFB, OH 45433-7817

**ABSTRACT.** Honeycomb composites are increasingly finding utility in a variety of environments and applications, such as aircraft structural components, flight control components, radomes, etc. In-service and environmental stresses can produce unwanted flaws that adversely affect the structural integrity and functionality of these composites. These flaws may be in the forms of disbonds, delaminations, impact damage, crushed honeycomb, moisture intrusion, internal cracks, etc. There are several nondestructive testing (NDT) methods that may be used to inspect these composites for the presence and evaluation of these flaws. Such NDT methods include X-ray computed tomography, near-field millimeter wave, shearography, and ultrasonic testing. To assess the capabilities of these methods for honeycomb composite inspection, two honeycomb composites panels were produced with several embedded flaws and missing material primarily representing planar disbonds at various levels within the thickness of the panels and with different shapes. Subsequently, the aforementioned NDT methods were used to produce images of the two panels. This paper presents the results of these investigations and a comparison among the capabilities of these methods.

**Keywords:** honeycomb composite, microwave and millimeter wave, nondestructive testing (NDT), shearography, through-transmission ultrasound, X-ray computed tomography.

**PACS:** 81.70.Cv, 81.70.Ex, 81.70.Fy, 81.70.Tx.

## INTRODUCTION

Honeycomb composites are widely used in various applications and industries including the aerospace industry. Components such as flight control surfaces and radome structures are two examples in which composite skin-composite honeycomb may be utilized. Flight control surfaces are used to control in-flight stability and motion, while radomes are typically designed to protect radar or communication systems from

undesired environmental effects while minimally influencing the system performance. Therefore, any subsurface flaws in a honeycomb composite radome can significantly degrade the performance of the system. Hence, there is a great need to inspect the honeycomb composites routinely and assess their electrical and structural integrities.

Composites with honeycomb cores and glass fiber-reinforced polymer (GFRP) skins can be inspected, for subsurface flaws using, a variety of nondestructive testing (NDT) methods. Such methods include X-ray computed tomography (CT), near-field microwave/millimeter techniques, shearography, and through-transmission ultrasonic testing (TTU) [1], [2].

In this paper, the detection and resolution capabilities of the X-ray CT, near-field millimeter wave techniques, shearography, and TTU to inspect honeycomb-core composite panels with several embedded defects are investigated. To this end, these NDT methods were used to capture images for these panels. Based on the captured images and the manifestation of the detected flaws, the efficacy of each of the used NDT methods for such application is assessed.

## **SAMPLES DESCRIPTION**

Two honeycomb composites panels (1"-thick and 0.5"-thick) each with one side bonded with a thin GFRP laminar skin and the other side bonded with a thin carbon reinforced (CFRP) skin. Unfortunately, there were no drawings or information provided on how these panels were constructed, therefore, the NDT results were used to gain insight on the defects inside the samples. The panels appear to be produced with several embedded defects made out of thin polymer sheets (i.e., Teflon tape, plastic, paper, etc.) and missing honeycomb/skin material. The embedded defects primarily represented planar disbonds, crushed core, and delaminations at various heights within the thickness of the panels and with different shapes.

The first panel (Panel #1) is a 1" -thick honeycomb sample produced by stacking two 0.5"-thick honeycomb layers on top of one another with a mid-thickness composite septum separating the honeycomb layers. The second panel composite (Panel #2) was similarly manufactured except that it had a single layer of 0.5"-thick honeycomb core. Figure 1 shows pictures of these panels.

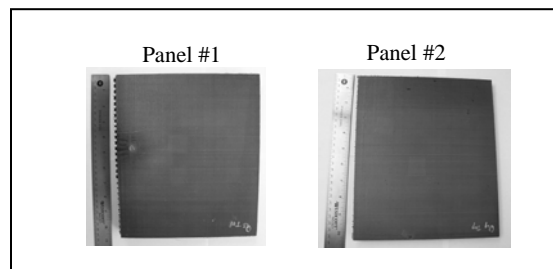


**Figure 1: Pictures of the two honeycomb composite panels.**

## **X-RAY COMPUTED TOMOGRAPHY (CT)**

X-ray computed tomography works on the basis of conventional x-ray NDE techniques. The conventional X-ray source has a small focal spot size. Apertures at the source and detector limit the X-rays to a plane passing through the specimen. As the X-rays pass through the specimen they are attenuated by the specimen material along ray paths between the X-ray source spot and each detector element. The attenuated X-rays are detected by a linear array of detectors located on the other side of the specimen. The specimen is rotated until measurements are made throughout 180 degrees of rotation. The resulting measurements are manipulated by a computer according to a reconstruction algorithm to produce a two-dimensional map of the X-ray attenuation in the irradiated cross section. The resulting data correspond to point-by-point density values in thin cross sections of the specimen, in effect allowing three-dimensional imaging of the internal structure when successive transverse sections are produced. For this investigation, the CT slices were taken at 1mm intervals.

Figure 2 shows selected image slices of Panel #1 obtained using X-ray CT. The slices show different images as a function of depth within the panel thickness. As shown in the Figure 2, there are four subsurface flaws of different shapes appearing at the upper right-hand corner of the core-GFRP skin interface slice. A rectangular flaw is detected at the upper right-hand corner of the next slice shown. The image corresponding to the slice at the middle of the core shows one additional flaw in the panel septum. Finally, the core-CFRP skin interface slice reveals two rectangular flaws around the middle of the top portion of the panel (as well as the words “NDI TEST” engraved in the honeycomb at that depth).

The X-ray CT sliced images of Panel #2 are shown in Figure 3. It is evident that most of the detected subsurface flaws are concentrated in the upper portion of the panel. The image slice corresponding to the core-GFRP skin interface shows four rectangular flaws at the upper left-hand side. Meanwhile, the middle slice indicates the presence of one flaw at the upper right hand corner. The image slice corresponding to the core-CFRP skin interface shows two additional rectangular flaws.

In summary, the X-ray CT detected at least 21 different subsurface flaws in Panel #1 and 14 subsurface flaws in Panel #2. This method is clearly well-established, capable and provides detailed information both spatially and through the panel depth. Therefore, these X-ray CT results will be primarily used subsequently to benchmark the other NDT techniques considered herein. This is partially due to the fact that the panel schematics were not available at the time of these investigations. However, due to the high resolution capabilities of this method (in 3-D) these results are used in the place of the missing panel schematics.

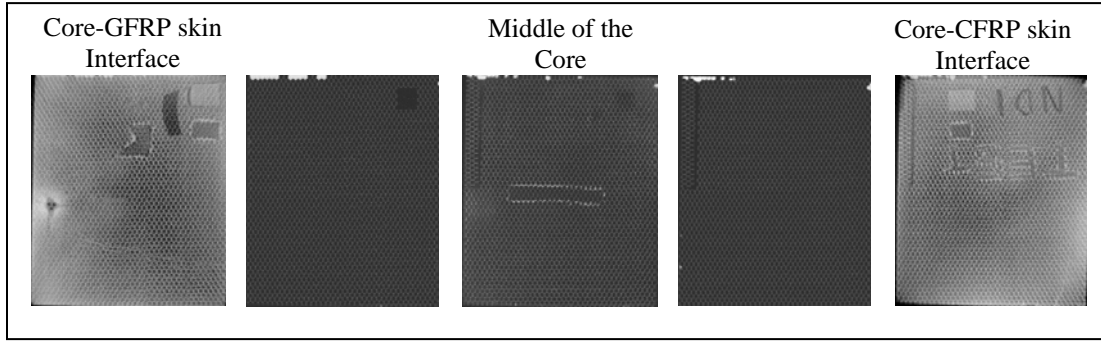


Figure 2: X-ray CT image slices of Panel #1.

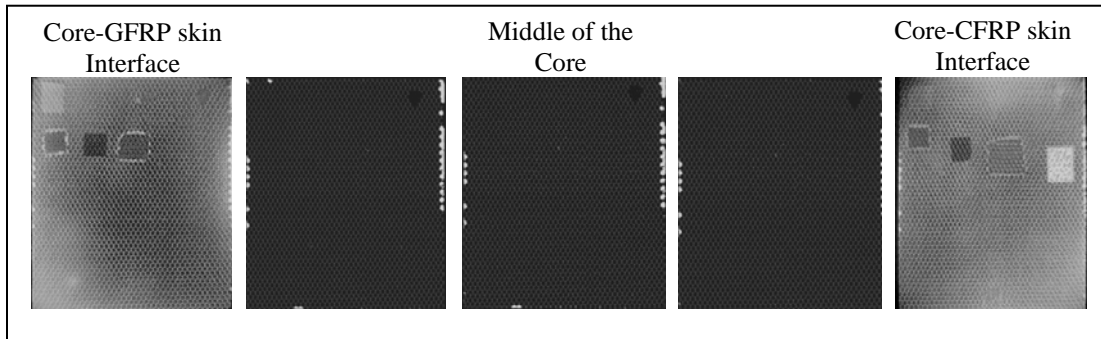


Figure 3: X-ray CT image slices of Panel #2.

## NEAR-FIELD MILLIMETER WAVE TECHNIQUE

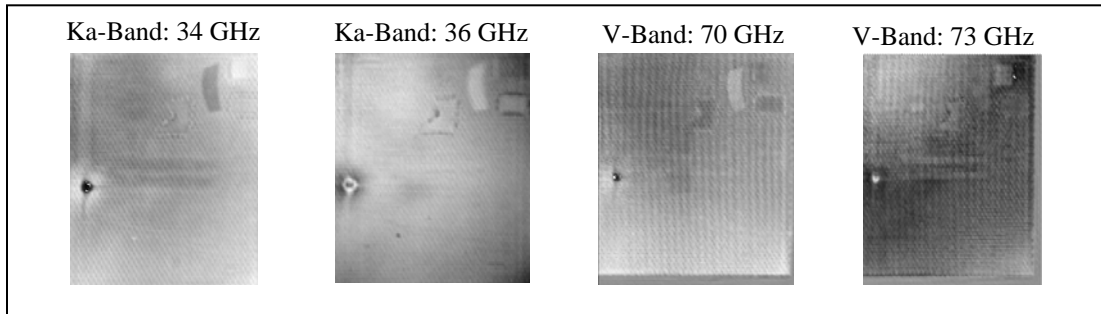
The suitability of microwave/millimeter wave methods for honeycomb composite inspection stems from the fact that these composites are in the family of low permittivity and low loss materials. Consequently, millimeter wave signals easily penetrate inside these composites and interact with their interior structure [3]-[5]. In general, a flaw in the honeycomb composite is considered as a discontinuity in the dielectric properties of that medium. Millimeter wave-based NDT systems are particularly appealing for this application since these waves are sensitive to minute dielectric property discontinuities in a composite host material.

Panels #1 and #2 were imaged using several near-field millimeter wave reflectometers, using open-ended rectangular waveguide probes, operating over a relatively wide range of frequencies from 26.5 GHz to 75 GHz (mainly Ka- and V-bands). The rectangular waveguide probe was used to irradiate the samples from the GFRP skin side and receive the reflected signal. Millimeter wave signals do not penetrate through the CFRP skin, however they go through a total reflection at this interface when inspecting from the GFRP side. The waveguide probe raster scanned the panels in one plane, the *imaging plane*, in a C-scan fashion where it also picked up the reflected signal from the panel. The images were then formed as 2D intensity maps in which the intensity is a function of the reflected signal power and/or phase at each sampling point in the imaging plane [4]. For the Ka-band probe (26.5-40 GHz), it was found that flangeless rectangular waveguides yielded better images (i.e., less interference between the would-be flange and the panel skin). Since the panels are made of low loss dielectric materials (e.g., glass and honeycomb), the reflectometers were designed to be more sensitive to the

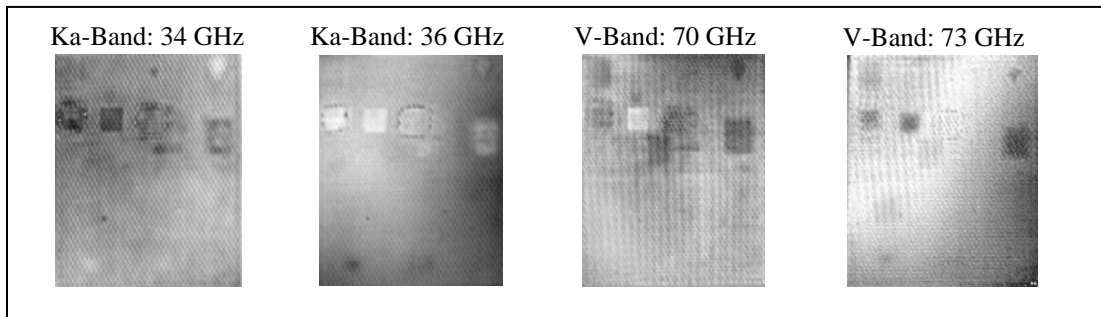
phase variations in the reflected signal. This was accomplished by heterodyning the reflected signal with a reference signal [2].

Figure 4 shows the corresponding images (raw) of Panel #1 at two different frequencies in the Ka- and V-band frequency ranges. The strong and localized indication near the left edge of the panel is due to a surface flaw and does not correspond to any of the embedded flaws. When comparing these images with those shown in Figure 2, it is interesting to note that specific embedded flaws are detected and their relative spatial allocations and sizes are also clearly indicated. Furthermore, flaws at different depths are detected at the same time and in the same imaging process (unlike slices in the X-ray CT images). This is an important practical issue. Generally, the V-band images show some flaws which are not a clearly indicated in the Ka-band images.

Figure 5 shows a set of similar images obtained from Panel #2. The same conclusions are made for this panel as those for Panel #1. Additionally, some overlapping flaws were also detected in these images (the 34 GHz and 70 GHz images). Comparing these results with those shown in Figure 3, it is clear that many of the flaws were detected even those that overlapped through the panel depth. Once again, the V-band images provided higher flaw detectability and resolution compared to the Ka-band images.



**Figure 4: Millimeter wave images of Panel #1 obtained at 34 GHz, 36 GHz, 70 GHz, and 73 GHz.**



**Figure 5: Millimeter wave images of Panel #2 obtained at 34 GHz, 36 GHz, 70 GHz, and 73 GHz.**

## **SHEAROGRAPHY**

The type of Shearography used in this investigation is referred to phase stepped shearography and is based on the principles of laser speckle and optical interferometry. The images are generated by allowing the monochromatic, coherent light to interfere on the test sample and produce a reference speckle pattern. When the sample is stressed, this interference will produce a fringe pattern that differs from the reference speckle

pattern, which represents displacement between adjacent points. The stressed state image and reference image are subtracted to indicate material strength.

The images shown in Figure 6 - 8 were formed using different vacuum stress state values. Figure 6 shows the Shearography images of Panel #1 obtained using various vacuum pressure values applied at the GFRP skin side. Four subsurface flaws of different sizes are apparent at the top right corner of the panel. Hence, this technique detected 8 out of the 22 flaws detected in this panel. The exact shapes of the flaws, however, are not clear in the obtained image with respect to other NDT methods used in this investigation.

The same pressure values were used to capture shearography images of Panel #2. The pressure was applied at the GFRP side first then at the CFRP side. Figure 7 and Figure 8 show the resulting images, respectively. Collectively, both images indicated the presence of 8 out of 15 flaws. Again, the shapes of the detected flaws are not well defined in these images.

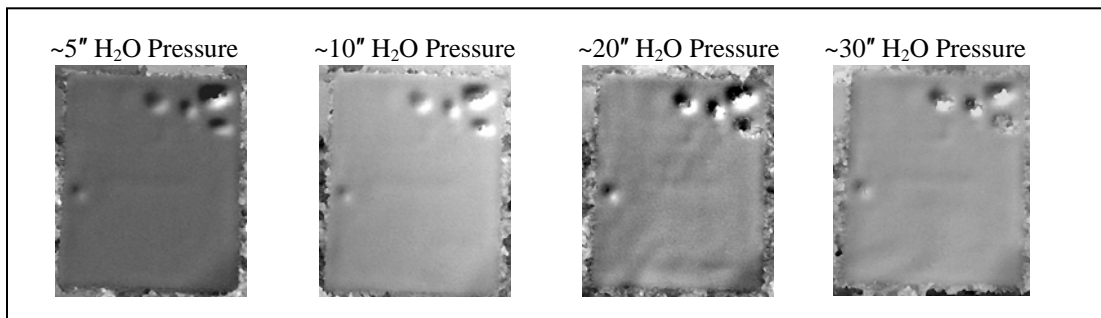


**Figure 6: Shearography images of Panel #1 using different pressure values applied at the GFRP skin side.**

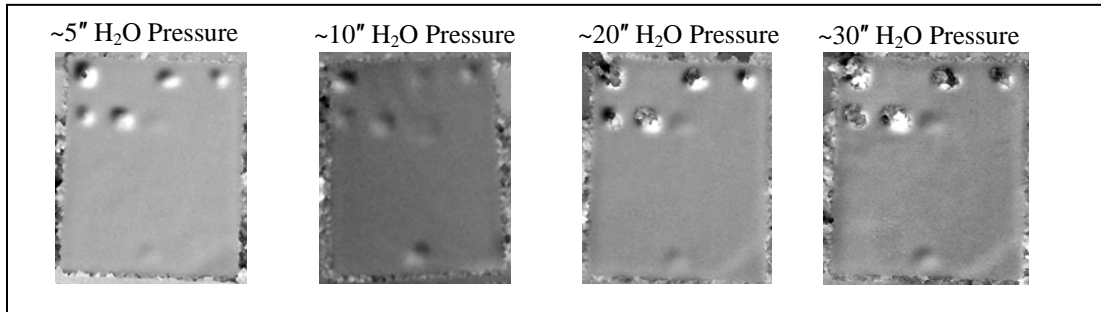


**Figure 7: Shearography images of Panel #2 using different pressure values applied at the GFRP skin side.**

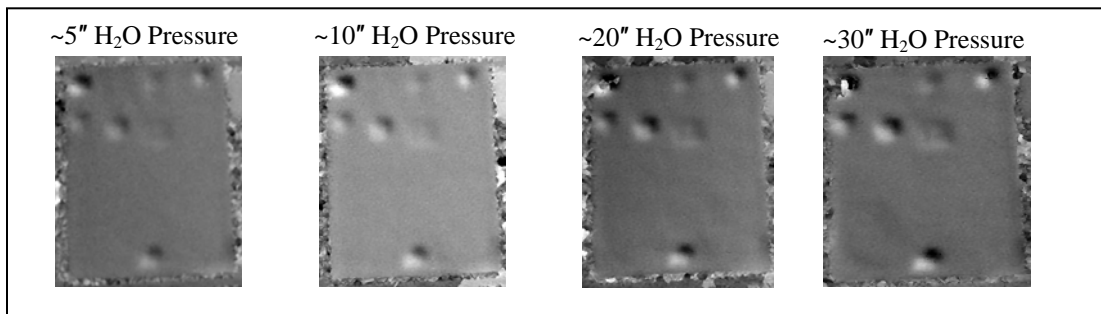


**Figure 8: Shearography images of Panel #2 using different pressure values applied at the CFRP skin side.**



## THROUGH-TRANSMISSION ULTRASOUND

Through-Transmission Ultrasound (TTU) is a widely-used and traditional technique for inspecting honeycomb components for bonding defects. TTU relies on a couplant and involves the use of two piezoelectric transducers aligned coaxially on both sides of the samples. One transducer is used to transmit the ultrasonic energy through the sample, and the other transducer is used to receive or detect any sonic energy that is not attenuated by the sample. For this particular investigation, the information collected by the receiving transducer was peak amplitude data only.

Figure 9 shows the TTU images of Panels #1 and #2 obtained at 5 MHz with scanning resolution of 0.01". The image obtained from Panel #1, distinctly indicates the presence of 16 out of the 22 subsurface flaws. The flaws in the upper right hand corner are blurred and difficult to individually distinguish. Unfortunately, the sound propagation is restricted in a TTU inspection through a double layer honeycomb sample with a septum, such as Panel #1. This is due to the misalignment of the honeycomb layers, in which the sound energy depends on to optimally carry the energy through the sample. As for Panel #2, the obtained image clearly shows 8 subsurface flaws out of possible 15. Furthermore, the shapes of the detected flaws can be readily determined in the image.



**Figure 9: Through-transmission ultrasound images of Panels #1 and #2.**

## SUMMARY

Two composites panels with honeycomb cores (1"-thick and 0.5"-thick) each with one side covered with a thin GFRP skin and the other side with a thin CFRP skin were produced with several embedded planar flaws. Four NDT methods (X-ray CT, near-field millimeter wave, shearography and through-transmission UT) were used to inspect these panels by producing their images. Since the schematics of the panels were not available at the time of testing, the CT image slices were used as the primary reference.

X-ray CT method produced high resolution images of the embedded flaws. Moreover, it provided flaw depth information. The major disadvantages of this technique are that it is slow, expensive, bulky, and not suitable for on-line real-time inspection. Furthermore, the ionizing nature of the radiation limits its use and requires strict precautions to be implemented during use.

The images obtained by the millimeter wave probes revealed, with high spatial resolution, most of the subsurface flaws. The shapes of the flaws were clearly evident in the raw near-field images as well. Since the utilized near-field probes were uncalibrated and were produced at single frequencies, it was not possible to retrieve the flaw depth

information quantitatively. The relative signatures of the flaws in the obtained images, however, indicated the existence of flaws at different depths, i.e., overlapping flaws. Overall, the results obtained by this method were comparable to those of the X-ray CT (with the exception of flaw depth evaluation). This method is non-contact, high resolution, and through-depth detection of flaws utilizing portable, inexpensive, and relatively small probes which can be easily incorporated into existing scanning platforms is readily possible. The millimeter wave probes do not need a couplant, and they can facilitate fast and on-line real-time inspection. This method is limited by its sensitivity to the standoff distance variations and inability to penetrate through the CFRP skin.

The X-ray CT images indicated the presence of most defects in both samples, but there was an indication in each panel from the Shearography and TTU images that did not show up in the X-ray CT. These indications not seen in the X-ray CT images were interpreted as pure disbonds or delaminations because there is no apparent material density change. The lateral resolution provided by this technique was shown to be the best among the four methods. The Shearography method generated images much faster than any other NDI modality in this investigation. Shearography's high detection capability and simple equipment in addition to the fact that it does not require couplant makes it appealing for this type of application. On the other hand, the disadvantages of this method include its low lateral resolution and expensive equipment. Finally, it requires the application of a stress to the inspected parts.

As shown by the obtained images for both samples, the through-transmission ultrasound testing (TTU) method offered the lowest detection capability. However, its lateral resolution was higher than the Shearography. The advantages of the TTU are that it produces images with a relatively high resolution, facilitates real-time on-line inspection, can be easily incorporated into the existing platforms, and uses simple inspection equipment. The applicability of this method, however, is impaired by the strong internal scattering by the honeycomb core. TTU is a non-contact method, but it requires couplant and access to both sides of the panel. A major disadvantage of Shearography and TTU are the defects at the same planar location but at different depths within test samples will show up as only one defect. There were many defects within these panels that were masked by others. Additionally, if inserts are well-bonded to the adjacent composite skin layers and have similar sound propagation characteristics, these flaws will not be detected by Shearography or TTU. Table 1 gives a qualitative comparison among these four techniques.

The data interpretations of the samples were focused on the X-ray CT data because of its 3-D nature and its resolution with respect to all the techniques in this investigation. Based on the interpretation of the images generated from each of the techniques, there were 22 flaws in Panel #1. There appears to be three flaws (3 inserts) in the GFRP skin, five flaws (1 insert, 1 skin mill out at the skin-honeycomb interface, 3 honeycomb hogout removals) at the GFRP-honeycomb interface, one flaw (1 honeycomb hogout) through the honeycomb layer on the side of the GFRP, one flaw (1 honeycomb hogout) at the septum, one flaw (1 honeycomb hogout) through the honeycomb layer on the side of the CFRP skin, ten defects (9 honeycomb hogouts – one for each letter in “NDI TEST”, 1 insert). In addition, there was a single flaw in Panel #1 that appears to be a disbond or a delamination in the UT and the Shearography images that was not detected by X-ray CT.

There appears to be 15 flaws in Panel #2: two flaws (2 inserts) in the GFRP skin, five flaws (1 insert, 1 skin mill out at the skin-honeycomb interface, and 3 honeycomb hogout removals) at the GFRP-honeycomb interface, one flaw (1 honeycomb hogout) through the honeycomb core, five flaws (1 insert, 1 skin mill-out, and 3 honeycomb hogouts), one flaw (1 insert) CFRP skin. Like Panel #1, there was also a single flaw in Panel #2 that appears to be a disbond or a delamination in the UT and the Shearography images that was not detected by X-ray CT. The detection results from each modality are shown in Table 1.

**Table 1. Summary of detection and resolution attributes of the four NDT methods.**

	<b>Detection (Number of Flaws)</b>		<b>Lateral Resolution</b>
	<b>Panel #1 (22 flaws)</b>	<b>Panel #2 (15 flaws)</b>	
<b>X-Ray CT</b>	21	14	High
<b>Near-Field Millimeter Wave</b>	12	13	High
<b>Shearography</b>	8	8	Low
<b>Through-Transmission UT</b>	16	8	Moderate

## ACKNOWLEDGEMENT

This work has been supported by a grant from the Air Force Research Laboratory (AFRL) under contract no. FA8650-04-C-5704, in conjunction with the Center for Aerospace Manufacturing Technologies (CAMT) at the University of Missouri-Rolla (UMR).

## REFERENCES

1. P. J. Shull (Ed), *Nondestructive Evaluation, Theory, Techniques, and Applications*, Marcel Dekker, Inc., NY, 2001.
2. Zoughi, R., *Microwave Non-Destructive Testing and Evaluation*, Kluwer Academic Publishers, the Netherlands, 2000.
3. N. Qaddoumi, R. Zoughi, and G.W. Carriveau, "Microwave detection and depth determination of disbonds in low-permittivity and low-loss thick sandwich composites," *Research in Nondestructive Evaluation*, vol. 8, no. 1, pp. 51-63, 1996.
4. Qaddoumi, N., S.I. Ganchev, G. Carriveau and R. Zoughi, "Microwave imaging of thick composites with defects," *Materials Evaluation*, vol. 53, no. 8, pp. 926-929, August, 1995.
5. Greenawald, E.C., L.J. Levenberry, N. Qaddoumi, A. McHardy, R. Zoughi and C.F. Poranski, "Microwave NDE of impact damaged fiberglass and elastomer layered composites," *Proc. of the 26<sup>th</sup> Annual Review of Progress in Quantitative Nondestructive Evaluation*, vol. 19B, pp. 1263-1268, July 1999.